AGE (2014) 36:733–748
DOI 10.1007/s11357-014-9617-4

Consequences of age on ischemic wound healing in rats: altered antioxidant activity and delayed wound closure

Andrea N. Moor · Evan Tummel · Jamie L. Prather · Michelle Jung · Jonathan J. Lopez · Sarah Connors · Lisa J. Gould

Received: 22 August 2013 / Accepted: 7 January 2014 / Published online: 21 January 2014

Abstract Advertisements targeted at the elderly population suggest that antioxidant therapy will reduce free radicals and promote wound healing, yet few scientific studies substantiate these claims. To better understand the potential utility of supplemental antioxidant therapy for wound healing, we tested the hypothesis that age and tissue ischemia alter the balance of endogenous antioxidant enzymes. Using a bipedicled skin flap model, ischemic and non-ischemic wounds were created on young and aged rats. Wound closure and the balance of the critical antioxidants superoxide dismutase and glutathione in the wound bed were determined. Ischemia delayed wound closure significantly more in aged rats. Lower superoxide dismutase 2 and glutathione in non-ischemic wounds of aged rats indicate a basal deficit due to age alone. Ischemic wounds from aged rats had lower superoxide dismutase 2 protein and activity initially, coupled with decreased ratios of reduced/oxidized glutathione and lower glutathione peroxidase activity. De novo glutathione synthesis, to restore redox balance in aged ischemic wounds, was initiated as evidenced by increased glutamate cysteine ligase. Results demonstrate deficiencies in two antioxidant pathways in aged rats that become exaggerated in ischemic tissue, culminating in profoundly impaired wound healing and prolonged inflammation.

Keywords Aging · Ischemia · Glutathione · Rat · Superoxide dismutase · Wounds

Electronic supplementary material The online version of this article (doi:10.1007/s11357-014-9617-4) contains supplementary material, which is available to authorized users.

A. N. Moor (✉) · L. J. Gould
Department of Molecular Pharmacology and Physiology, University of South Florida,
12901 Bruce B. Downs Blvd, MDC 8, Tampa, FL 33612, USA
e-mail: amoor@health.usf.edu

A. N. Moor · E. Tummel · J. L. Prather · M. Jung · L. J. Gould
Department of Plastic Surgery, James A. Haley Veterans Hospital,
Tampa, FL 33612, USA

E. Tummel · J. L. Prather · M. Jung · J. J. Lopez · S. Connors · L. J. Gould
Department of Surgery, University of South Florida,
Tampa, FL 33612, USA

Introduction

Wound repair in the elderly has previously been characterized as "impaired," but it is not clear how, or if, chronological age alone impacts the wound healing process. Increased proteolysis and degradation of the extracellular matrix, prolonged inflammation (with altered ratio of mature to immature macrophage populations), delayed re-epithelialization and neovascularization of the wound bed, impaired angiogenesis beneath the wound bed, and impaired fibroblast migration have all been demonstrated to some extent in aged mouse, rat, and human studies (Ashcroft et al. 1997a, b, 1998; Swift et al. 2001; Soybir et al. 2012). All wounds, but particularly chronic wounds, exhibit localized tissue hypoxia. As people age, the number of comorbid illnesses that result

in tissue ischemia increases, further complicating wound healing in these individuals. Both clinical and laboratory data support the hypothesis that aging results in an aberrant response to ischemic stress, with altered gene expression, impaired response to exogenous growth factors, and broad changes in signal transduction pathways (Mogford et al. 2004; Mustoe et al. 2006; Wu et al. 1999).

It is well established that low concentrations of reactive oxygen species (ROS) activate cell signaling pathways required for wound healing and that extracellular matrix remodeling depends on the delicate balance between superoxide dismutase (SOD), glutathione (GSH), and nitric oxide (NO) (Sen 2003). SOD is the first and most important line of defense against superoxide anions ($O_2^{\cdot -}$). This family of isozymes rapidly converts $O_2^{\cdot -}$ to hydrogen peroxide in a highly compartmentalized system (Zelko et al. 2002). SOD2 is the primary defense against ROS produced during aerobic respiration. Although transcription of SOD2 is increased by inflammatory cytokines, the enzyme is inactivated by specific tyrosine nitration and therefore is vulnerable to prolonged oxidative stress (MacMillan-Crow et al. 1998).

Hydrogen peroxide generated from the reduction of $O_2^{\cdot -}$ by SOD is converted to water and oxygen by the oxidation of sulfhydryl GSH catalyzed by glutathione peroxidase (GPx) and by recycling of glutathione disulfide (GS-SG) to GSH by glutathione reductase (GSR). In this reaction, reducing equivalents are provided by GSH, a key nonprotein thiol that maintains cellular redox integrity. In addition to recycling, GSH homeostasis is maintained by de novo synthesis of GSH (Chen et al. 2010; Franklin et al. 2009; Seelig et al. 1984; Tu and Anders 1998). Age-associated declines in GSH level have been reported in brain and liver (Liu et al. 2004; Liu and Choi 2000) and reduced expression of the catalytic subunit of glutamate cysteine ligase (Franklin et al. 2009) was noted in the soleus muscle of aged rats under stress (Chen et al. 2010). Thus, a marked reduction in GSH synthesis, from either dysfunctional recycling or inadequate de novo synthesis, could lead to disruption of the balance between SOD and GSH in aging skin. In fact, heat stress has been shown to cause oxidative damage in aged rats because of wide fluctuations in SOD activity coupled with diminished GSH levels (Morrison et al. 2005).

The process of ROS removal within the wound bed is not well understood nor is it known how the age-related shift in cellular redox status to an oxidative profile affects the ability of mammals to respond to stresses such as wounding or tissue ischemia. We have found that single antioxidant supplementation is ineffective (preliminary data). Therefore, we hypothesized that ischemic stress in the aged animal leads to a combined deficit of the endogenous antioxidants that culminates in oxidative injury and excessive inflammation. In this study we utilized our validated rat ischemic wound model to isolate the condition of tissue hypoxia from other co-morbidities that may contribute to delayed healing in the elderly. Based on preliminary data, we focused specifically on the endogenous antioxidant enzyme deficits as the mechanism responsible for the aberrant response to ischemic stress.

Methods

Animal procedures

All animal procedures were approved by the Animal Care and Use Committee at the University of South Florida and abided by all requirements of the Animal Welfare Act and the Guide for Care and Use of Laboratory Animals. Healthy 6 (young) and 23–24 months (aged) male Fisher 344 rats (National Institute on Aging, Bethesda, MD) were utilized to create an ischemic wound model. The model, adapted from our work with Sprague–Dawley rats (Gould et al. 2005), takes into account the increased sensitivity of the aged Fisher 344 rat to cutaneous ischemia and a longer median lifespan of about 31 months (males) versus 24–25 months for Sprague–Dawley rats. Full-thickness excisional wounds were created in the center of a 10.5× 3.5-cm flap (ischemic wounds) with a 6-mm punch biopsy and wound healing followed for 2, 5, 7, 10, 14, and 21 days. Control (non-ischemic) full-thickness wounds were created on either side of the ischemic flap for comparison. At the time of wounding (Day 0) and upon harvest, six rats from each group (young and aged) were anesthetized, ischemic and non-ischemic wounds were digitally photographed, and wound sizes were determined. Two non-ischemic and two ischemic wounds from each animal were divided in half, with one part of the wound preserved in 10 % buffered formalin for histology and immunohistochemistry and the other three parts snap frozen in liquid nitrogen, stored separately at −80 °C, and subsequently used for analysis of antioxidant protein levels and activity,

mRNA and GSH/GS-SG (reduced sulfhydryl GSH to oxidized disulfide GSH) ratios.

Histopathology

Wounds fixed with 10 % buffered formalin for 24 h were embedded in paraffin and sectioned at 4 μm. Serial sections were deparaffinized, rehydrated, and washed in distilled water in preparation for hematoxylin and eosin (H&E) staining. Digital brightfield images of the wound beds at 4× and 40× were obtained using a Nikon (TE2000) inverted microscope coupled with a Q-Imaging Retiga 2000R camera and Nis Elements (Advanced Research version 3.20.01) software.

PCR array

Wound tissues were homogenized and total RNA extractions were performed using the FastRNA pro system (MP Biomedicals, Solon, OH). RNA was DNase-treated to remove contaminating genomic cDNA and further purified using RNeasy clean-up columns (Qiagen, Valencia, CA). For PCR array experiments, RNA from four rats per group (young non-ischemic, young ischemic, aged non-ischemic, and aged ischemic) from day 7 were pooled giving four test samples, which were run 2× to generate appropriate statistics. The rat oxidative stress and antioxidant defense RT^2 profiler™ PCR array (SABiosciences-Qiagen) was used to quantify the expression of antioxidant, ROS metabolism, and oxygen transporter genes. One microgram of RNA from each group was reverse transcribed into cDNA using the RT^2 First Strand kit (SABiosciences-Qiagen). SYBR Green ROX™ qPCR master mix (SABiosciences-Qiagen) was used together with the reverse-transcribed cDNA for QT-PCR and aliquoted into the PCR array and run on a 7900HT QT-PCR machine (Applied Biosystems-Life Technologies). Dissociation (Melting) curves were acquired at the end of each PCR run. Data was collected using SDS 2.1 ABI Prism software (Applied Biosystems; Life Technologies). Threshold cycle (C_t) values were exported to a Web-based PCR array analysis spreadsheet: http://sabiosciences.com/pcrarraydataanalysis.php (SABiosciences-Qiagen) that utilizes the $\Delta\Delta C_t$ method to calculate fold changes for each gene. The housekeeping gene Rplp1 was used for normalization as its C_t value was consistent across our four samples over the replicate runs. A fourfold regulation (up or down) in gene expression was used as the threshold and only genes of interest that matched these criteria were selected for further validation.

Wound tissue lysates for protein electrophoresis, Western blot, ELISA, and GPx activity

Wound tissues stored at −80 °C were trimmed to remove superficial eschar and underlying panniculus carnosus muscle. The remaining skin was weighed, minced with a razor blade and homogenized using a FastPrep®-24 (MP Biomedicals, Solon, OH) tissue homogenizer in tissue lysis buffer containing 10 mM Tris–HCl, pH 7.4, 150 mM NaCl, 1 % Triton X-100, 2 mM PMSF, and a protease inhibitor cocktail (Pierce, Rockford, IL). Following centrifugation at 14,000×*g* for 15 min, the supernatant was removed, sonicated briefly, centrifuged, and assayed for protein content using the Pierce BSA™ protein assay kit (Pierce, Rockford, IL). Tissue lysates were stored at −80 °C until analysis. Lysates were thawed, mixed 1:4 with 5× sample buffer (0.3 M Tris–HCl, 5 % (*w*/*v*) SDS, 50 % (*v*/*v*) glycerol, 100 mM DTT, and a pink tracking dye; ThermoScientific, Pierce Biotechnology, Rockford, IL) boiled for 3 min, loaded (5 μg/lane) onto 4–20 % gradient precast gels and transferred to Protran BA 83 nitrocellulose membrane (Whatman®, Dassel, Germany). Membranes were blocked for 1 h in 5 % skim milk powder in 1× TBS-T, pH 7.5 (TBS with 0.1 % Tween 20), rinsed in TBS-T, and incubated overnight at 4 °C with mouse anti-glutamate cysteine ligase-modifier subunit (GCLM) antibody (ab55436; Abcam, Cambridge, MA) at a dilution of 1:1,000 or with rabbit anti-GSR (ab16801) at 1:1,000. The membranes were then washed in TBS-T and incubated for 1 h at room temperature with either an HRP-conjugated goat anti-rabbit IgG (H+L) or an HRP-conjugated anti-mouse IgG at a dilution of 1:3,000. Bands were visualized with Pierce® ECL Western Blotting Substrate (Pierce, Rockford, IL) and Kodak BioMax Light film (Carestream Health, Inc, Rochester, NY). Relative quantities (volume (intensity*mm^2)) of protein were determined using a BioRad imager (BioRad, Hercules, CA) and densitometry software (QuantityOne, version 4.6.3, BioRad, Hercules, CA). Data are expressed as percent (mean±SD; n=5–6/group).

ELISA for SOD and GPx1

SOD1 (cytosolic), SOD2 (mitochondrial), and GPx1 protein levels were measured using rat-specific ELISA kits (USCN Life Sciences, Inc and Cedarlane

Laboratories USA, Inc, Burlington, NC). Briefly, purified standards, blanks, and samples (100 μl of wound tissue lysate; n=6–8/group) were incubated in microplate wells precoated with monoclonal anti-SOD1, SOD2, or GPx1 antibody for 2 h at 37 °C. Wells were emptied (not washed) and a biotin-conjugated polyclonal antibody specific for SOD1, SOD2, or GPx1 was added for 1 h at 37 °C. Following washing of the wells (3×) an avidin conjugated to horse radish peroxidase solution was added to the wells and incubated for 30 min at 37 °C. Following washing of the wells (5×), a TMB substrate solution was added to the wells and the plate incubated for 15–25 min at 37 °C. The reaction was stopped by the addition of sulphuric acid (stop solution) and the absorbance was read spectrophotometrically at a wavelength of 450 nm. Standard curves were generated by plotting the log of the optical density values of the standard (x-axis) against the known concentration of the standard (y-axis). Values were normalized to the protein concentration of each sample. Data are expressed as mean±SD (n=6–8).

SOD activity—sample preparation

Wound tissues stored at −80 °C prepared as described above were minced on ice in 300 μl of SOD buffer containing 20 mM HEPES, pH 7.2, 1 mM EGTA, 210 mM mannitol, and 70 mM sucrose. The tissue was homogenized in a matrix A tube using a FastPrep®-24 (MP Biomedicals, Solon, OH) in a final volume of 500 μl. Samples were centrifuged at 1,500×g for 20 min at 4 °C. The supernatants were transferred to clean eppendorf tubes and sonicated briefly (2 s) on the lowest setting to break open any remaining intact cells. Total protein concentration was determined prior to centrifugation at 15,000×g for 40 min at 4 °C. The supernatants (cytosolic fraction) were removed to clean eppendorf tubes. The mitochondrial pellets were resuspended in 60 μl of SOD buffer and sonicated for 2 s. The cytosolic (SOD1) and mitochondrial (SOD2) samples were assayed for protein concentration as described previously.

SOD activity

SOD 1 and SOD 2 activities were measured using a kit that utilizes a tetrazolium salt for detection of superoxide radicals generated by xanthine oxidase and hypoxanthine (Cayman Chemical Co. Ann Arbor, MI). One unit of SOD is defined as the amount of enzyme needed to exhibit 50 % dismutation of the superoxide radical. Briefly, SOD standards (0–0.25 U/ml activity) and samples were added to the wells and each received 200 μl of diluted radical detector. The reactions were initiated by the addition of xanthine oxidase to the wells and incubating for 20 min at room temperature. Absorbance was read at 460 nm. Average absorbance was calculated and then the linearized rate (LR) for each standard was derived. The linearized SOD standard rate was calculated as a function of final SOD activity (units per milliliter) for a typical standard curve. SOD activity of the samples (cytosolic=SOD1 and mitochondrial=SOD2) was obtained using the equation obtained from the linear regression of the standard curve by substituting the LR for each sample. Results were the normalized to the weight (mg) of starting wound tissue. Data are represented as mean±SD (n=4–6.)

Total GSH and ratio of GSH-GS-SG

A GSH detection kit (Cayman Chemical Co., Ann Arbor, MI) was used to measure micromolar quantities of GS-SG (equivalent to total GSH) in wound tissue lysates. Wound tissues were weighed, minced in 1XPBS, and added to a MPLysing Matrix A tube (MP Biomedicals, Solon, OH) containing 1XPBS on ice. Tissues were homogenized using the FastPrep®-24, sonicated for 5 s on ice and centrifuged for 20 min at 10,000×g at 4 °C. Supernatants were transferred to 0.5 ml Amicon® ultra centrifugal filters (30 K; Millipore Corp., Billerica, MA) and centrifuged for 10 min at 14,000×g at 4 °C, and the flow through was frozen at −80 °C for later analysis. Samples did not require deproteination. For determination of total GSH, a standard curve was prepared using GS-SG. Under the assay conditions, GS-SG is immediately reduced to GSH thereby providing the necessary standard. The determination of GS-SG, exclusive of GSH, was performed by derivatizing GSH with 2-vinylpyridine (Sigma, St. Louis, MO) for 1 h at room temperature. A separate standard curve prepared using 2-vinylpyridine was incubated for the same amount of time as the samples (1 h). Absorbance was measured at 405 nm and endpoint readings were obtained after 25 min incubation at room temperature in the kit substrate solution. The average of duplicate absorbance readings were recorded for standards and samples (n= 6–8) and background was subtracted. Corrected absorbance for each standard was plotted as a function of the concentration of GS-SG or total GSH and linear

regression curves were generated. Sample absorbance was then used in a curve fit analysis to obtain the average micromolars per well of GS-SG or total GSH and finally normalized to wound tissue weight (in grams). Data are presented as mean±SD; n=5–8 samples/group and time point.

GPx activity

GPx activity was measured indirectly by a coupled reaction with GR (Cayman Chemical Co. Ann Arbor, MI). Briefly, GS-SG, produced upon reduction of hydroperoxide by GPx is recycled to its reduced state by GR and NADPH. Oxidation of NADPH to $NADP^+$ is accompanied by a decrease in absorbance at 340 nm. In conditions where GPx activity is rate limiting, the rate of decrease in the A_{340} is directly proportional to the GPx activity in the sample (Paglia and Valentine 1967). Background (non-enzymatic), positive control (bovine erythrocyte GPx), and samples (20 μl of wound tissue lysate) were added to a microplate along with 120 μl of assay buffer (50 mM Tris–HCl, pH 7.6, and 5 mM EDTA) and 50 μl of co-substrate (NADPH, GSH, and GR). Reactions were initiated by the addition of cumene hydroperoxide to all the wells and the absorbance was read once every minute at 340 nm for 8 min. Absorbance values were plotted as a function of time to obtain the slope (rate) of the linear portion of the curve. GPx activity was then calculated by determining the rate of ΔA_{340}/min (slope) for the background and subtracting this rate from that of the samples. The following formula was then used to calculate GPx activity: ΔA_{340}/min÷ 0.00373 μM^{-1} (0.19 ml÷0.02 ml)=nmol min^{-1} ml^{-1}, where 0.00373 is the NADPH extinction coefficient (adjusted for the pathlength of the solution in the well which is 0.6 cm) used to determine the reaction rate at 340 nm. Finally, GPx activity values were normalized to protein concentration (micrograms per microliter). Data are presented as mean±SD (n=6–8).

Statistical analysis

Data are presented as mean±SD. Student's unpaired t test, Mann–Whitney rank sum test, or one-way analysis of variance with post hoc comparisons performed using the Student–Newman–Keuls Method (normal data) were used to determine the statistical significance between groups using SigmaStat® version 3.5 (Systat Software, Inc., Point Richmond, CA). P values of less than 0.05 were considered significant. PCR array and qPCR data are represented as fold change with a P value of less than 0.05 considered significant.

Results

Wound closure is delayed with aging and ischemia in Fisher rats

Wound area was quantified from digital images (Fig. 1a) of the wounds at day (D) 2, 5, 7, 10, 14, and 21 in non-ischemic and ischemic groups (young and aged). The data are presented as a percentage of initial wound area (6 mm punch biopsy area=(Π) $r^2=3.14\times9=28.26$ mm^2) at D0 (Fig. 1b). Expectedly, ischemic wound healing in both groups is significantly delayed compared with non-ischemic wounds (young D2, P=0.039; D5–D10, P=<0.001; D14, P(exact)=0.004; aged D2: P=0.013; D5–10, P=<0.001; D14 P(exact)=0.002; and D21, P(exact)=<0.001). At approximately the midway point of healing, age differences became apparent and from D10-D21 ischemic wounds in aged rats were significantly larger than ischemic wounds in young rats (P=0.002; P=0.008; and P=0.006, respectively). No difference in wound area was observed between young and aged non-ischemic wounds at any time point.

Histopathology: ischemic wounds from aged Fisher rats are characterized by prolonged inflammation

Non-ischemic wounds from young and aged rats did not present with any significant gross morphological differences over the time course (Fig. 1a). Histologically, the non-ischemic wounds from young (see Online Resource 1a–c) and aged (Online Resource 1d–f) rats were similar in terms of amount of granulation tissue formation, inflammatory infiltrate (neutrophil and macrophage) clearance, re-epithelization, and epithelial thickness on days 10 through 21. The only apparent difference was at day 21 when non-ischemic wounds from young rats (see supplemental Fig. 1c versus f) showed slightly better remodeling of the dermis with new hair follicle development. Dermal fibroblasts in both young and aged were oriented parallel to the epidermis (see Online Resource 1, insets c and f).

Ischemic wounds overall (Fig. 2a–c (young), d–f (aged)) were characterized by less granulation tissue, high density of neutrophils and macrophages (especially

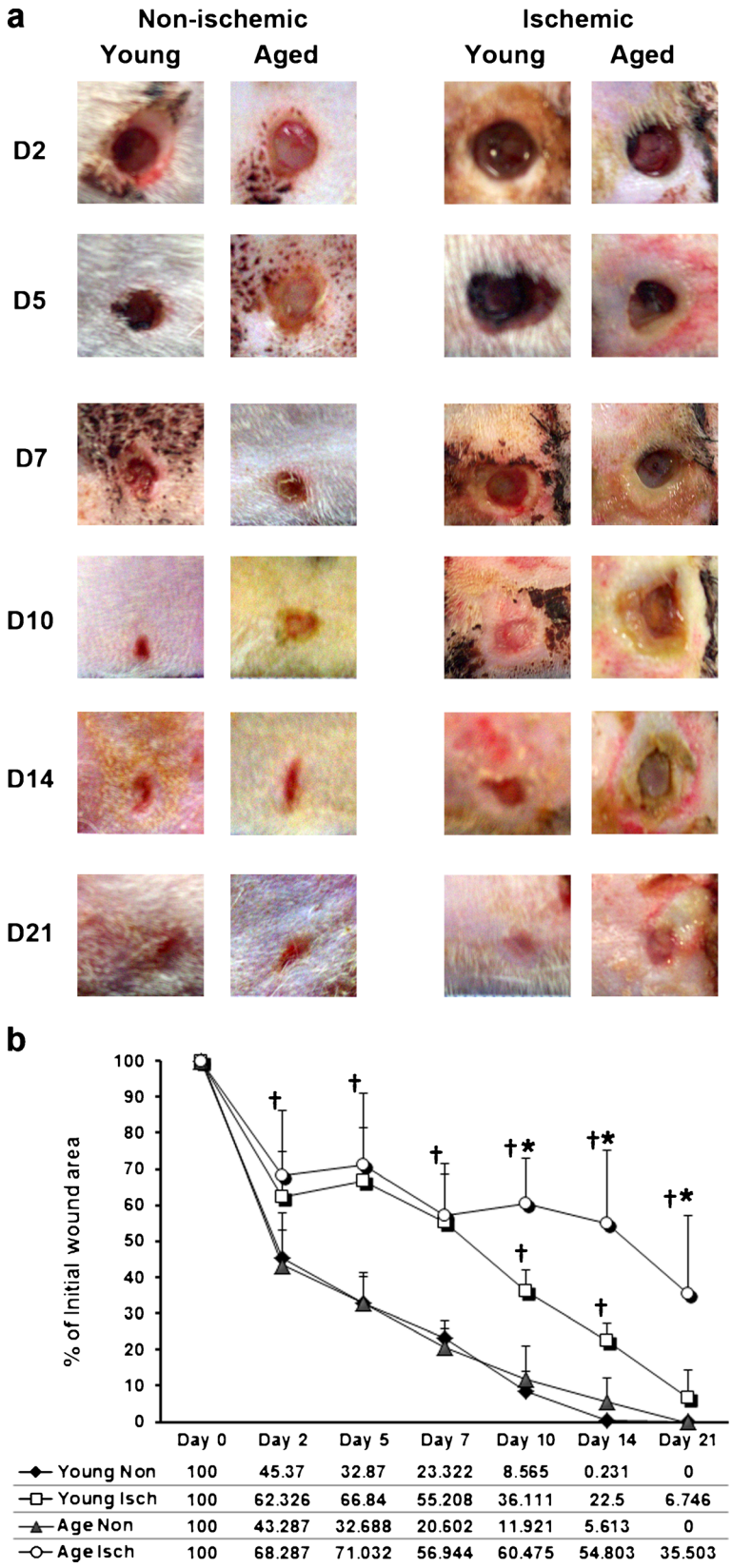

Fig. 1 Wound closure is delayed by ischemia and age in a Fisher 344 rat model. Wound area was quantified from digital images (**a**) of the wounds at day (*D*) 2, 5, 7, 10, 14, and 21 in non-ischemic and ischemic groups (young and aged). The data are presented as a percentage of initial wound area (6 mm punch biopsy area=(Π) r^2=3.14×9=28.26 mm^2) at D0 (**b**). Data are represented as percent (mean±SD), n=6–8/group. *Asterisk* represents significantly greater than non-ischemic group at the same time point; *dagger* represents significantly greater than the non-ischemic group (young and aged) at the same time point

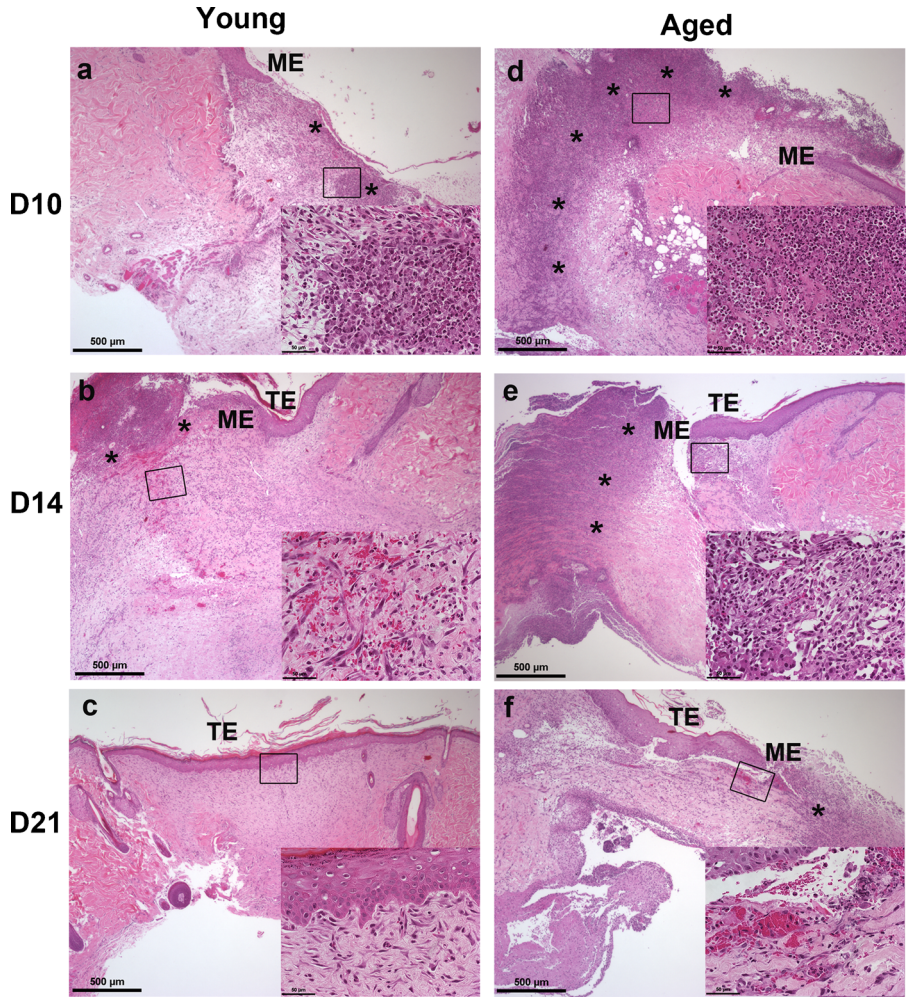

Fig. 2 Histopathology: ischemic wounds from aged Fisher rats are characterized by prolonged inflammation. Representative H&E staining of days 10, 14, and 21 ischemic (**a**–**c** young; **d**–**f** aged) wounds at 4× power and 40× insets (n=3–4 sections/group/time point). *Asterisk* indicates inflammatory infiltrate (neutrophils); *ME* migrating epithelial tongue, *TE* thickened epidermis. *Scale bars*=500 μm and 50 μM (*insets*)

in the ischemic wounds from aged rats (compare a and d) and reduced clearance of these inflammatory cells. Although small clusters of neutrophils (*) could be detected in ischemic wounds from young rats at days 10 and 14 (a–b), macrophages were the predominant cell type present in areas of the wound bed not covered by an epithelium. Dermal fibroblasts were observed from day 10 onward (insets a–c) as the dermis began to reorganize. Fibroblasts in the ischemic wounds of young rats were initially disorganized and did not become oriented parallel to the epidermis until day 21, much later than non-ischemic wounds from young or aged rats. In ischemic wounds from aged rats, neutrophils (*) were detected in high densities throughout the wound bed (inset in d) along with macrophages through day 14. Small pockets of neutrophils remained through day 21. Macrophages could also be seen throughout the granulation tissue and under the migrating epidermis at days 14–21 (e–f insets). Dermal fibroblasts were still disorganized at day 21 (inset in f). Compared with non-ischemic wounds, the epithelial tongue (ME) migration was markedly slower in ischemic wounds (days 10–14, a–b). This was particularly noticeable in ischemic wounds of aged rats (d–f), which still had not re-epithelialized by day 21 (f). The epithelium in ischemic wounds remained thickened through day 21 compared with non-ischemic wounds (see Online Resource 1).

Table 1 Oxidative stress PCR array data represented as fold regulation (up or down) of select antioxidant genes from isolated day 7 wound tissues

Abbrev. gene name	Gene name	Aged ischemic versus young ischemic	Aged ischemic versus aged non-ischemic	Young ischemic versus young non-ischemic	Aged non-ischemic versus young non-ischemic
SOD1	*Superoxide dismutase 1*	NC	NC	NC	NC
SOD2	*Superoxide dismutase 2*	NC	NC	NC	↓−5.02
Gpx1	*Glutathione peroxidase 1*	↓−5.17	NC	NC	NC
Gpx3	*Glutathione peroxidase 3*	↓−16.47	NC	NC	↓–4.38
Gpx6	*Glutathione peroxidase 6*	↑+4.88	NC	NC	NC
Gpx7	*Glutathione peroxidase 7*	↓-28.98	NC	NC	↓-5.82
Gpx8	*Glutathione peroxidase 8*	↓-15.21	NC	NC	↓-5.22
GSR	*Glutathione reductase*	NC	NC	NC	NC

[a] NC signifies no change

[b] ↓ Signifies down regulation while ↑ signifies up regulation of specific gene

Multiple antioxidant genes are downregulated by age alone

The oxidative burst produced by infiltrating neutrophils during the early inflammatory phase of wound healing results in ROS production and release into the wound bed. Based on the histologic findings that inflammation was prolonged in ischemic wounds, we examined an array of genes specific to oxidative stress and antioxidant defense at a time when we would expect the antioxidant response to be at its peak. Table 1 summarizes the PCR array data of select antioxidant genes from isolated day 7 wound tissues. No significant (over fourfold) changes in the selected genes were observed with ischemia compared with non-ischemia for both young and aged groups. However, SOD2 (mitochondrial), GPx3 (extracellular), GPx7 (a GPx precursor), and GPx8 (putative) were significantly downregulated with age in non-ischemic wounds compared with young non-ischemic wounds. Comparing ischemic wounds of young and aged, GPx1 (cytosolic and most abundant with preferred substrate hydrogen peroxide), GPx3, GPx7, and GPx8 were all significantly downregulated by age. In contrast GPx6 (found in olfactory epithelium and in embryonic tissues) was upregulated. GPx2 (found in gastrointestinal tissues), GPx5 (epididymal androgen-related protein), and GPx4 (cytosolic with preferred substrate lipid hydroperoxides) were all unchanged as expected. GSR was also unchanged.

SOD1 protein is differentially increased in ischemic wounds from young and aged rats without a parallel increase in SOD1 activity

Antioxidant SOD1 (cytosolic) protein levels and activity were measured in wound tissue total cell lysates and cytosolic fractions of wound tissue as an indirect measure of ROS, specifically superoxide anion, in the wound beds. SOD1 protein (measured by ELISA) was significantly elevated in ischemic wounds from young (Fig. 3a, top inset; days 5 (P=0.009), 7 (P=0.002), 10 (P=0.002) and 14 (P=0.015)) and aged (Fig. 3a, bottom inset; days 2 (P=0.035), 5 (P=0.008), 7 (P=0.004), 10 (P=0.010), 14 (P=0.004), and 21 (P=0.003)) rats at almost all time points compared with non-ischemic wounds. Ischemic wounds from aged rats also showed significantly higher SOD1 protein levels throughout the time course compared with ischemic wounds from young rats (Fig. 3a; day 2 (P=0.003), 7 (P=0.032), 10 (P=<0.001), 14 (P=<0.001), and 21 (P=0.017)). Despite increased SOD1 protein due to ischemia we were unable to detect differences in the SOD1 activity (U/mg) in ischemic wounds compared with non-ischemic wounds of young and aged rats (data not shown). SOD1 activity was not different in ischemic wounds from young compared with aged rats (Fig. 3b).

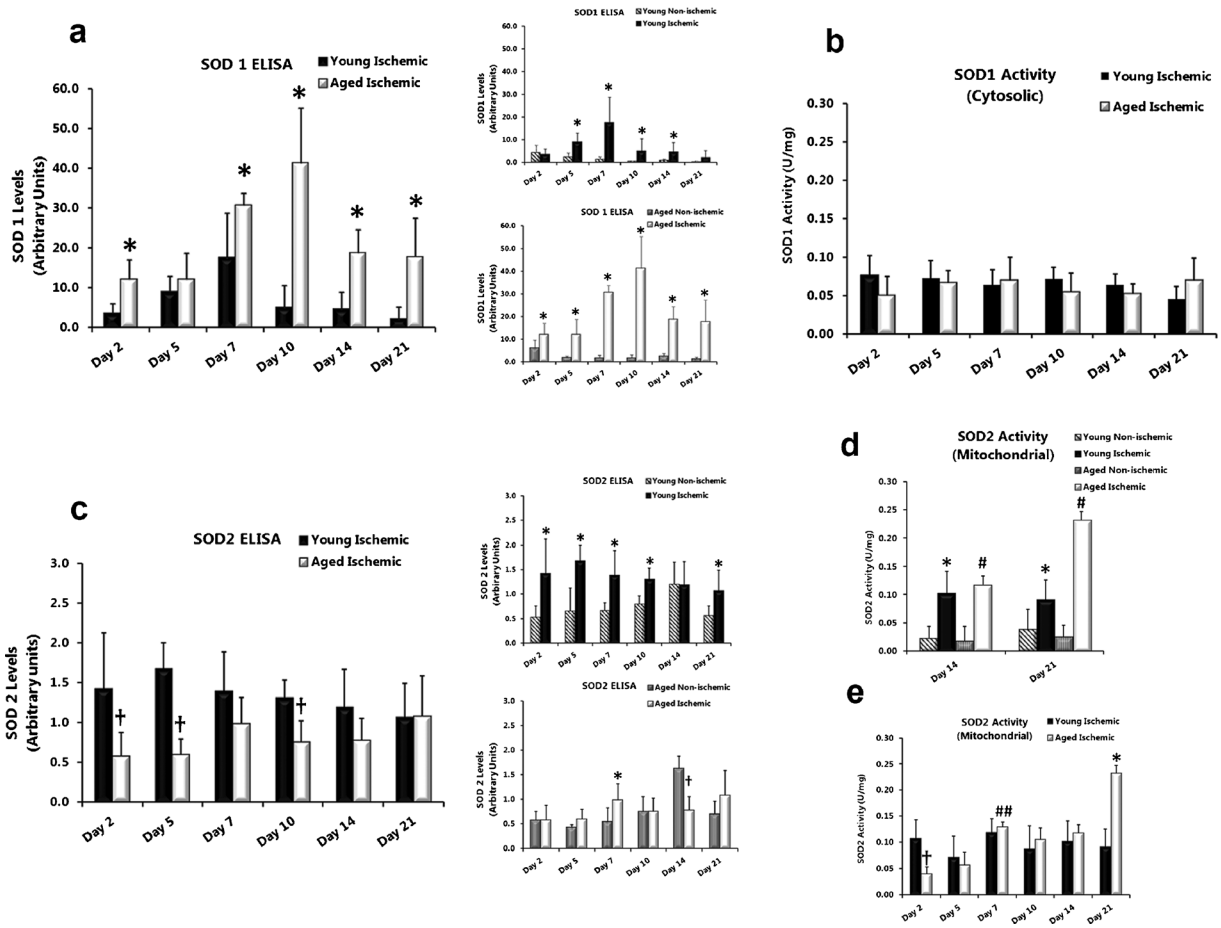

Fig. 3 SOD1 protein is differentially increased in ischemic wounds from young and aged rats without a parallel increase in SOD1 activity. **a** (*insets*) SOD1 (soluble) protein levels were measured in wound homogenates using a rat-specific ELISA kit, monoclonal antibody to SOD1, and absorbance read at 450 nm. Values were normalized to the protein concentration of each sample. Data are expressed as mean±SD; n=6–8. *Asterisk*, significantly higher (P<0.05) than young ischemic (**a**) or non-ischemic (*insets*). **b** SOD1 enzymatic activity (units per milligramme of wound tissue) in ischemic wound tissue from young and aged rats. Data are expressed as mean±SD; n=4–8. **c** (*insets*) SOD2 protein is decreased in ischemic wounds from aged rats during early phases of healing with corresponding lower SOD2 activity. SOD2 (mitochondrial) protein levels in wounds were measured using a rat-specific ELISA kit as described above but using a monoclonal SOD2 antibody. Data are expressed as mean±SD; n=6–8. *Asterisk*, significantly higher (P<0.05) than non-ischemic; (*Dagger*) significantly lower than aged non- ischemic (**c**, *bottom inset*) and young ischemic (**c**). **d** SOD2 enzyme activity (units per milligramme of wound tissue) in young and aged non-ischemic wounds versus ischemic wounds at days 14 and 21. Data are expressed as mean±SD, n=4–8. *Asterisk*, significantly higher (P<0.05) than young non-ischemic; *number sign*, significantly higher than aged non-ischemic. **e** SOD2 activity levels over the time course in ischemic wounds from young and aged rats. *Dagger*, significantly lower than young non-ischemic; *number sign*, significantly higher than aged ischemic at days 2 and 5; *asterisk*, significantly higher than young ischemic

SOD2 protein is decreased in ischemic wounds from aged rats during early phases of healing with corresponding lower SOD2 activity

Antioxidant SOD2 (mitochondrial) protein levels and activity were measured in wound tissue total cell lysates and mitochondrial fractions as an indirect measure of mitochondrial ROS, specifically superoxide anion, in the wound beds. SOD2 protein (as measured by ELISA) was significantly elevated in ischemic wounds from young rats (Fig. 3c, top inset; days 2 (P=0.026), 5 (P=0.006), 7 (P=0.028), 10 (P=0.001), and 21 (P=0.036)) at most time points compared with non-ischemic wounds. Aside from a significant elevation at day 7 (P=0.041), ischemia did not change SOD2 protein levels in aged rats compared with non-ischemic (Fig. 3c, bottom inset). In ischemic wounds SOD2 protein was significantly lower in aged rats compared with

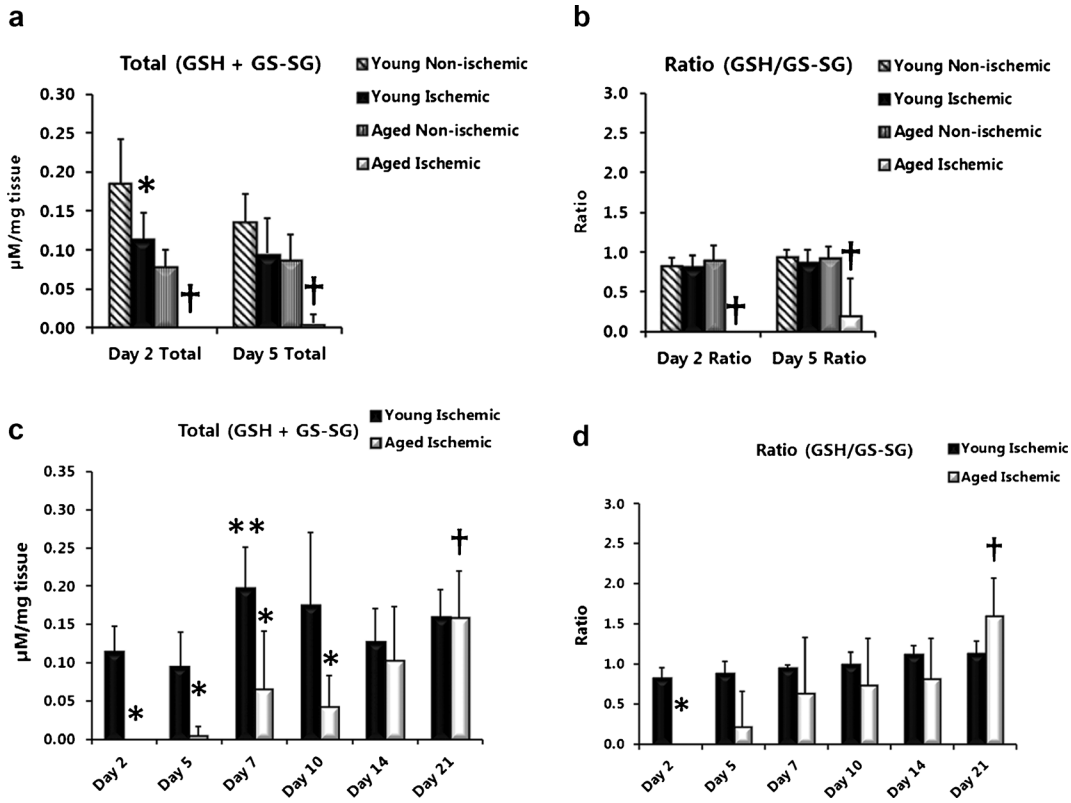

Fig. 4 Lower total glutathione (GSH+GS-SG) levels for an extended time and decreased ratios of GSH/GS-SG distinguish aged from young ischemic wounds. Total glutathione levels (GSH+GS-SG, micromolars per milligramme of wound tissue) (**a**) and ratios (GSH/GS-SG) (**b**) in non-ischemic and ischemic wound tissue lysates from young and aged rats. The combination of the sulfhydryl group of GSH and 5,5′-dithio-bis-2-(nitrobenzoic acid) produces 5-thio-2-nitrobenzoic acid, and its absorbance was read at 405–414 nm. Data are presented as mean±SD; n=5-8. *Asterisk*, significantly lower (P<0.05) than young non-ischemic; *dagger*, significantly lower than aged non-ischemic. **c** (GSH+GS-SG) levels and ratios (GSH/GS-SG) (**d**) in ischemic wound tissue lysates from young and aged rats. *Asterisk*, significantly lower than young ischemic; *double asterisk*, significantly higher than young ischemic days 2 and 5; *Dagger* in (**c**), significantly higher than aged ischemic day 10; *dagger* in (**d**), significantly higher than young ischemic

young rats (Fig. 3c) on days 2 (P=0.037), 5 (P=<0.001), and 10 (P=0.003). SOD2 activity in ischemic wounds from aged rats was initially low (Fig. 3e day 2; P=0.017) compared with ischemic wounds from young rats but increased significantly by days 7 (compare with days 2 (P=<0.001) and 5 (P=0.003) aged ischemic wounds). SOD2 activity in ischemic wounds (aged) paralleled low SOD2 protein levels at days 2 and 5 compared with ischemic wounds from young rats (Fig. 3c) and the increase in SOD2 protein at day 7 (Fig. 3c, bottom inset). By day 14, SOD2 activity in non-ischemic wounds from young and aged rats dropped significantly, whereas activity in the ischemic wounds was maintained (Fig. 3d). Lastly, SOD2 activity in ischemic wounds from aged rats increased significantly at day 21 (Fig. 3e; P=0.004) compared with ischemic wounds from young rats.

Lower total glutathione (GSH+GS-SG) levels for an extended time and decreased ratios of GSH/GS-SG distinguish aged from young ischemic wounds

To investigate the GSH antioxidant system's capacity to neutralize hydrogen peroxide generated by SOD antioxidant activity, levels of total glutathione (GSH+GS-SG) and the ratio of reduced to oxidized glutathione (GSH/GS-SG) were measured in wound tissue lysates. During the early phase of wound healing (days 2 and 5), total GSH levels were significantly decreased in ischemic wounds compared with non-ischemic wounds (Fig. 4a) in both young (day 2; P=0.0034) and aged (day 2; P=0.004 and day 5; P=<0.001) rats. However, lower ratios of GSH/GS-SG were only observed in ischemic wounds from aged rats (Fig. 4b days 2 and day 5; P=0.004 and P=0.052. This age difference was clearly observed

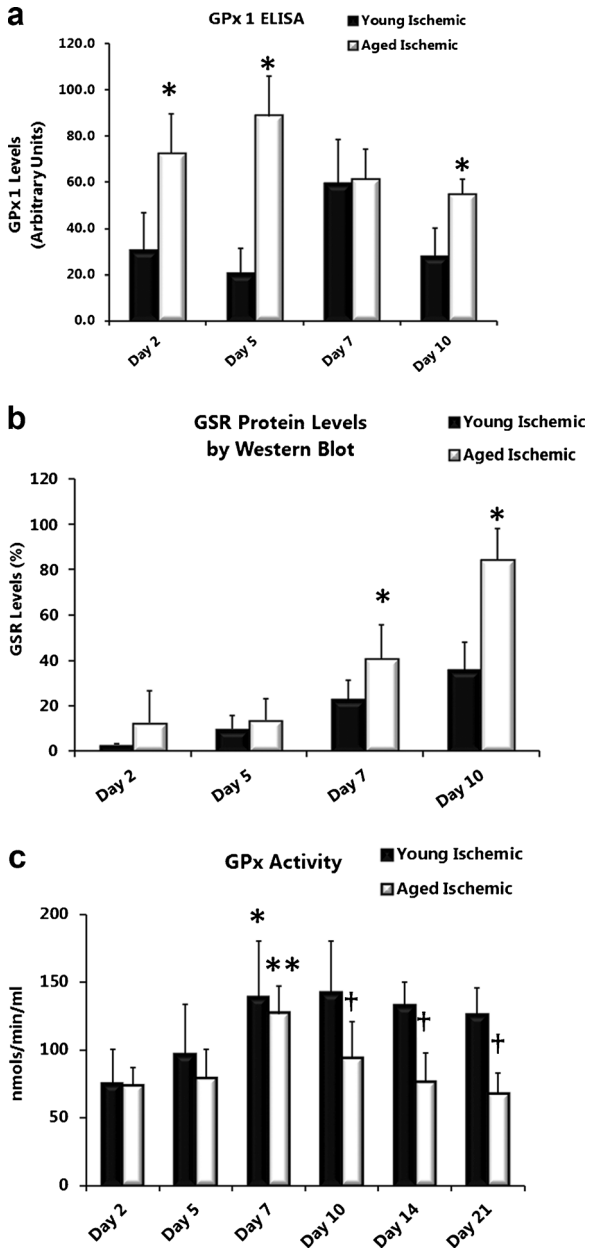

Fig. 5 Age differentially affects GPx1 and GSR protein levels in ischemic wounds. GPx1 (**a**) and GSR (**b**) protein levels in ischemic wound tissue lysates from young and aged rats analyzed by ELISA and Western, blot respectively. Data are presented as mean ±SD; n=6–8 (ELISA) and n=5–6 (Western blot analysis). *Asterisk*, significantly higher (P<0.05) than young ischemic. GPx activity is lower in ischemic wounds from aged rats. **c** GPx activity (nmols/min/ml) in ischemic wound tissue lysates from young and aged rats. (*Asterisk*) significantly higher than young ischemic day 2; (*Double Asterisk*) significantly higher than aged ischemic day 2 and day 5; (*Dagger*) significantly lower than young ischemic

when total GSH levels between ischemic wounds from aged and young rats were compared (Fig. 4c) over the full time course. Total GSH was significantly lower in ischemic wounds from aged rats (day 2, P=0.008; day 5, P=0.003; day 7, P=0.007 and day 10, P=0.008) compared with young rats and remained lower for a much longer time (through day 10) not showing a recovery until day 14 with a significant increase reached by day 21(day 21 versus day 10, P=0.008). By contrast, ischemic wounds from young rats showed significant increases in total GSH levels by day 7 (day 7 versus day 5, P=0.010; day 7 versus day 2, P=0.017). The GSH/GS-SG ratio was significantly lower in ischemic wounds from aged rats (Fig. 4d day 2, P=0.008) compared with young rats but did attain levels close to those of young rats by day 7. Ratios remained steady in ischemic wounds from young rats despite increases in total GSH levels. Also of note was the significant increase in the ratio of GSH/GS-SG in the aged at day 21 (P=0.043).

Age differentially affects GPx1 and GSR protein levels in ischemic wounds

Levels of GPx1 and GSR, responsible for the conversion of GSH (substrate) to GS-SG and the recycling of GS-SG back to GSH, were quantified in wound lysates. GPx1 protein levels (by ELISA) were significantly elevated in ischemic wounds from aged rats compared with young rats (Fig. 5a day 2, P=0.016; day 5, P=<0.001, and day 10, P=0.001 and through day 14-data not shown). Unlike GPx1 protein levels, GSR protein (by Western blot) was almost undetectable until day 7 in ischemic wounds (and non-ischemic wounds-data not shown) from both young and aged rats (Fig. 5b). By day 7, GSR was elevated in ischemic wounds from aged rats compared with young rats (Fig. 5b days 7, P=0.038 and 10, P=<0.001). GSR declined similarly in ischemic wounds from both young and aged rats thereafter (data not shown).

GPx activity is lower in ischemic wounds from aged rats

Although there was no significant age difference in GPx activity (nanomoles per minute per milliliter) from non-ischemic wounds, GPx activity did trend lower in these wounds from aged rats from days 5 through 21 (data not shown). Ischemic and non-ischemic wounds paralleled each other with GPx activity steadily increasing to a maximum by day 7 (non-ischemic data not shown) (Fig. 5c; (young) day 7 versus day 2, P=0.020; (aged)

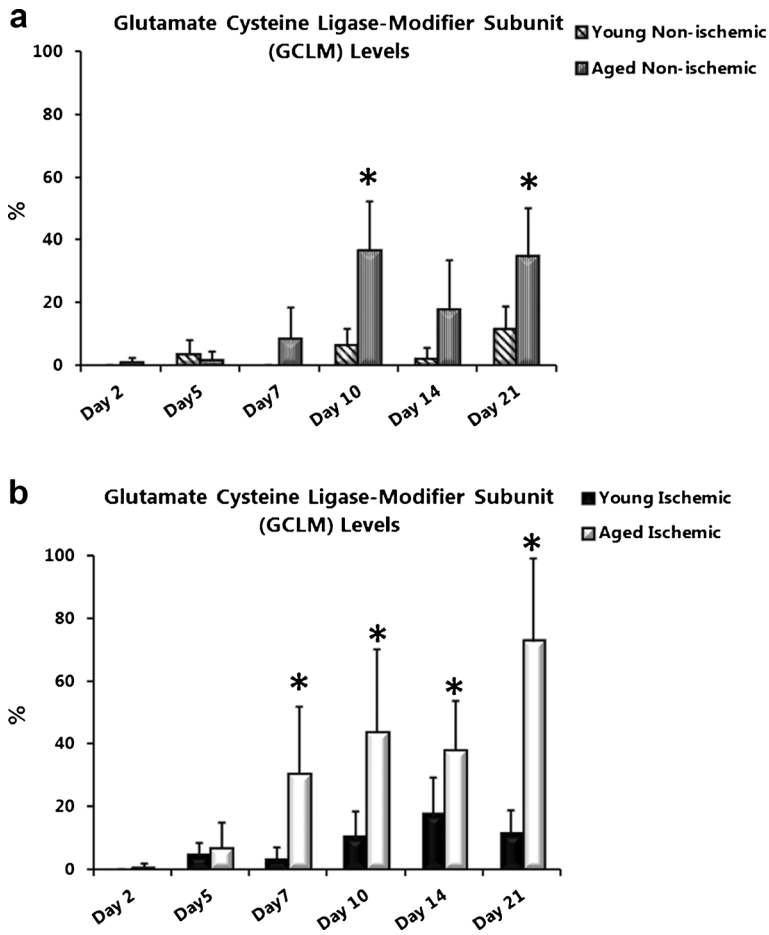

Fig. 6 Glutamate cysteine ligase-modifier subunit (GCLM) protein levels are increased with age and ischemia. Quantification of the modifier subunit of GCL (GCLM) in **a** non-ischemic and **b** ischemic wounds from young and aged rats. Band density was quantified after Western blotting and data are represented as percent mean±SD; n=5–6. *Asterisk* significantly higher than young non-ischemic in (**a**) and young ischemic in (**b**)

day 7 versus days 2 and 5, P=<0.001 and P=0.005). A decline in GPx activity characterized the remaining time course (day 10 through 21) with GPx activity significantly lower in ischemic wounds from aged compared with young rats (Fig. 5c; day 10, P=0.032; day 14, P=0.002; and day 21, P=<0.001)

Glutamate cysteine ligase-modifier subunit protein levels are increased with age and ischemia

One of the mechanisms responsible for increasing the ratio of GSH to GS-SG is the de novo synthesis of GSH. We examined GCLM protein levels, in wound lysates from non-ischemic and ischemic wounds. GCLM levels were almost undetectable in non-ischemic wounds from young and aged rats until day 10 when a significant increase was observed in non-ischemic wounds from aged (Fig. 6a; day 10, P=0.003; day 21, P=0.015) compared with young rats. In ischemic wounds from aged rats GCLM was significantly elevated from day 7 through day 21 compared with young rats (Fig. 6b; day 7, P=0.004; day 10, P=0.024; day 14, P=0.028; and day 21, P=0.002).

Discussion

The goal of this study was to identify targets for future interventional studies and wound therapies in elderly patients with ischemic wounds. To accomplish this goal, we studied the processes of ROS removal (via SOD and GSH antioxidant defense systems) that occur when advanced age is combined with tissue ischemia. It has been suggested that the age-associated decline in cellular function is due to the cumulative effects of low-level chronic oxidative stress generated by endogenously produced ROS (Sohal et al. 1994). Although ROS are

required for many aspects of wound healing, with aging there are increased mitochondrial and endoplasmic reticulum (ER) generated ROS, resulting in oxidative damage to nuclear and mitochondrial proteins, DNA and lipids. Proteins of the electron transport chain and (ER) chaperones sustain the most damage, resulting in nitration and carbonylation (Choksi et al. 2004). Oxidative damage to the mitochondrial genome accelerates ROS production, leading to a perpetual cycle of increased damage to macromolecules, more ROS and consequent mitochondrial dysfunction (Szczesny et al. 2004). This results in a state of chronic oxidative stress by virtue of advanced age alone, in the absence of external factors. Recently, Soybir et al., using an incisional wound model in rat, showed that ROS (detected by both luminol and lucigenin) in non-ischemic wounds from aged rats were significantly elevated up to 14 days after wounding (Soybir et al. 2012).

Previous studies using the rabbit ischemic ear model have demonstrated that age and ischemia are additive, resulting in profoundly impaired wound healing and a lack of response to exogenous growth factors (Bonomo et al. 2000; Wu et al. 1997, 1999). More recently, using a rat ischemic ear model, Mogford et al. confirmed a significant delay in wound healing when advanced age is combined with ischemia and demonstrated that ischemia alters the expression of more genes (both up and downregulated) in aged rats than in young (Mogford et al. 2004). In this study, we show that the delay in healing of excisional, ischemic wounds in aged rats is accompanied by a shift, early in the healing process, in cellular redox status towards an oxidative profile with a low ratio of GSH/GS-SG. Based on these results we propose that dysfunction of the antioxidant defense enzymes results in aberrant (ROS) signaling with age. As the endogenous redox system of the older animal becomes overwhelmed, the ability to respond to additional stressors, i.e., ischemia, is impeded. While ROS levels were not measured directly in this study, impaired wound healing was demonstrated grossly and histologically, with the divergence in wound closure between young and aged becoming apparent at day 10, accompanied by a prolonged inflammatory response in which both neutrophils and macrophages persist through day 21 in aged ischemic wounds.

Unlike the few previous studies that examined either ROS production or gene expression during non-ischemic and/or ischemic wound healing our study demonstrates several key deficiencies in the antioxidant response system due to age alone. First and foremost is a deficiency of SOD2. This mitochondrial antioxidant enzyme has been shown to be essential for cell viability and to regulate cell growth. Although SOD2 acts as both an antioxidant (removal of $O_2^{\cdot-}$) and a pro-oxidant (creation of hydrogen peroxide), this enzyme regulates the mitochondrial redox state. Changes in ROS resulting from SOD2 have been shown to elicit adaptive cellular responses from other cellular compartments, including cell cycle regulation and transcriptional regulation of nuclear genes encoding mitochondrial proteins (Kim et al. 2005). We show that SOD2 gene transcription is reduced in non-ischemic wounds of the aged compared with young rats, indicating a basal deficit in the low stress state. Under ischemic stress, SOD2 protein expression is induced in the young but not in the aged rat wounds. The lack of induction is greatest early, when control of the inflammatory response would be most important. We believe that this lack of response sets up a cycle of increased neutrophil infiltration with generation of additional ROS, resulting in cell death thereby attracting more neutrophils. Finally, our data show that SOD2 activity is induced early in young rat wounds but does not increase substantially in the aged ischemic wounds until day 21. We believe that this finding, although detrimental for wound healing, is consistent with the evolutionarily conserved mechanism in which product inhibition has been shown to control SOD2 activity, protecting mitochondria from overproduction of hydrogen peroxide (Davis et al. 2004). Specifically, as discussed later, aged ischemic wounds are severely deficient in GSH until day 14. Once this hydrogen peroxide-removing capacity is restored SOD2 activity increases.

Although the SOD isoenzymes all catalyze the same reaction, their subcellular location is important to physiological function. For example, overexpression of SOD1 does not rescue the lethal phenotype of SOD2 knockout mice (Copin et al. 2000). In this study we show that SOD1 protein expression is induced by ischemia in both young and aged rats, but is much greater in the aged ischemic wounds throughout the time course. However, because it is located in the cytosol, SOD1 cannot make up for the SOD2 deficit. We found it perplexing that SOD1 gene expression does not parallel the induction in protein expression following ischemia in either age group of animals as compared with the same age group without ischemic injury. However, it is not unthinkable that various inflammatory cytokines and/or other feedback mechanisms in the ischemic

wound bed may be activating the SOD translational machinery without noticeable changes in SOD mRNA levels. The stability of the mRNA, although not tested in this study, could also provide an explanation and analyzing this aspect over the time frame of 5–10 days may give us more insight. Furthermore, we show discordance between SOD1 activity and protein levels, indicating that newly translated SOD1 protein may have become dysfunctional, likely due to nitration. Although nitrated proteins are usually targeted for ubiquitination with subsequent degradation, proteins with dual modifications, i.e., nitration and methylation of lysine may become inaccessible for other forms of post-translational modifications such as ubiquitination (Krueger and Srivastava 2006), thus delaying or preventing their degradation. These measurements were beyond the scope of the current study but may explain the discordance between protein and activity levels.

Both SOD1 and SOD2 are susceptible to inactivation by nitration when there are simultaneous increases in $O_2^{\cdot-}$ and NO resulting in formation of peroxynitrite ($ONOO^-$) (Demicheli et al. 2007). Indicative of peroxynitrite formation, we have detected maximal levels of 3-nitrotyrosine in the ischemic wound bed between days 7 and 10 (data not shown), when the discordance between enzyme activity and protein levels is the greatest. Without sufficient SOD activity to neutralize the $O_2^{\cdot-}$, peroxynitrite, a short lived, but highly reactive species will initiate lipid peroxidation (Radi et al. 1991), DNA strand breaks (Salgo et al. 1995a, b) and protein modification(s) including oxidation and nitration (Beckman and Koppenol 1996). In addition to the SOD isozymes, nitrated proteins have been demonstrated in cutaneous inflammation (Greenacre et al. 2002) and implicated in the regulation of matrix metalloproteinases (MMPs) during wound healing (Lizarbe et al. 2008).

As discussed above, SOD cannot function independently. An appropriate level of hydrogen peroxide is required to maintain intracellular redox homeostasis and promote cell growth. When exposed to excess hydrogen peroxide human dermal fibroblasts (HDFs) isolated from aged patients exhibit decreased viability, decreased phosphorylation of pro-survival kinases and an increased entrance into senescence compared with young HDFs (Gurjala et al. 2005). Glutathione homeostasis, the primary mechanism for hydrogen peroxide reduction, is maintained through a combination of de novo GSH synthesis, GSH oxidation (and autooxidation) and redox recycling. In this study, we show that aged non-ischemic wounds have less total glutathione (GSH+GS-SG) than young non-ischemic wounds, indicative of fewer reducing equivalents in the low stress state. This basal difference is magnified in the aged ischemic wounds, likely due to consumption of GSH, but "catches up" by day 14 as de novo synthesis is induced. We also demonstrate markedly reduced GPx1 transcription due to age alone that becomes magnified under ischemic stress (Table 1). Although GPx1 protein is expressed at significantly higher levels in aged ischemic compared with young ischemic wounds, the enzyme cannot function in the absence of GSH. Taken together, our data indicate that healing of ischemic wounds in aged rats is dependent upon induction of de novo GSH synthesis. Unique to the aged animals, the induction of GCLM starting at day 7 post-wounding restores the GSH pathway's hydrogen peroxide-reducing capacity, with subsequent increases in SOD2 and GSH recycling activity.

In summary, we have demonstrated a combined deficiency in the antioxidant defense because of aging that is magnified when subjected to ischemic stress. Our experimental results demonstrate a marked delay in healing of ischemic wounds in aged rats with a prolonged inflammatory response and dysregulation of SOD and GSH antioxidant defenses not previously identified using other ischemic wound models. This study clarifies why single antioxidant therapies fail and lays the foundation for interventional studies that simultaneously address the combined mitochondrial antioxidant enzyme deficit, getting us closer to our goal of highly targeted molecular therapies that will improve wound healing in the rapidly growing elderly population.

Acknowledgments This work was supported by a Veteran's Affairs Merit Award (BX09-002) to L. Gould. The authors would like to thank the University of South Florida Pathology Core Facility for the preparation of histological specimens. The authors declare no conflicts of interest for this work.

Disclaimer The contents of this manuscript do not represent the views of the Department of Veterans Affairs or the US Government.

References

Ashcroft GS, Horan MA, Ferguson MW (1997a) Aging is associated with reduced deposition of specific extracellular matrix components, an upregulation of angiogenesis, and an altered inflammatory response in a murine incisional wound healing model. J Invest Dermatol 108(4):430–437

Ashcroft GS, Horan MA, Herrick SE, Tarnuzzer RW, Schultz GS, Ferguson MW (1997b) Age-related differences in the temporal and spatial regulation of matrix metalloproteinases (MMPs) in normal skin and acute cutaneous wounds of healthy humans. Cell Tissue Res 290(3):581–591

Ashcroft GS, Horan MA, Ferguson MW (1998) Aging alters the inflammatory and endothelial cell adhesion molecule profiles during human cutaneous wound healing. Lab Invest 78(1): 47–58

Beckman JS, Koppenol WH (1996) Nitric oxide, superoxide, and peroxynitrite: the good, the bad, and ugly. Am J Physiol 271(5 Pt 1):C1424–C1437

Bonomo SR, Davidson JD, Tyrone JW, Lin X, Mustoe TA (2000) Enhancement of wound healing by hyperbaric oxygen and transforming growth factor beta3 in a new chronic wound model in aged rabbits. Arch Surg 135(10):1148–1153

Chen CN, Brown-Borg HM, Rakoczy SG, Ferrington DA, Thompson LV (2010) Aging impairs the expression of the catalytic subunit of glutamate cysteine ligase in soleus muscle under stress. J Gerontol A Biol Sci Med Sci 65(2):129–137

Choksi KB, Boylston WH, Rabek JP, Widger WR, Papaconstantinou J (2004) Oxidatively damaged proteins of heart mitochondrial electron transport complexes. Biochim Biophys Acta 1688(2):95–101

Copin JC, Gasche Y, Chan PH (2000) Overexpression of copper/zinc superoxide dismutase does not prevent neonatal lethality in mutant mice that lack manganese superoxide dismutase. Free Radic Biol Med 28(10):1571–1576

Davis CA, Hearn AS, Fletcher B, Bickford J, Garcia JE, Leveque V, Melendez JA, Silverman DN, Zucali J, Agarwal A, Nick HS (2004) Potent anti-tumor effects of an active site mutant of human manganese-superoxide dismutase. Evolutionary conservation of product inhibition. J Biol Chem 279(13): 12769–12776

Demicheli V, Quijano C, Alvarez B, Radi R (2007) Inactivation and nitration of human superoxide dismutase (SOD) by fluxes of nitric oxide and superoxide. Free Radic Biol Med 42(9):1359–1368

Franklin CC, Backos DS, Mohar I, White CC, Forman HJ, Kavanagh TJ (2009) Structure, function, and post-translational regulation of the catalytic and modifier subunits of glutamate cysteine ligase. Mol Aspects Med 30(1–2):86–98

Gould LJ, Leong M, Sonstein J, Wilson S (2005) Optimization and validation of an ischemic wound model. Wound Repair Regen 13(6):576–582

Greenacre SA, Rocha FA, Rawlingson A, Meinerikandathevan S, Poston RN, Ruiz E, Halliwell B, Brain SD (2002) Protein nitration in cutaneous inflammation in the rat: essential role of inducible nitric oxide synthase and polymorphonuclear leukocytes. Br J Pharmacol 136(7):985–994

Gurjala AN, Liu WR, Mogford JE, Procaccini PS, Mustoe TA (2005) Age-dependent response of primary human dermal fibroblasts to oxidative stress: cell survival, pro-survival kinases, and entrance into cellular senescence. Wound Repair Regen 13(6):565–575

Kim A, Murphy MP, Oberley TD (2005) Mitochondrial redox state regulates transcription of the nuclear-encoded mitochondrial protein manganese superoxide dismutase: a proposed adaptive response to mitochondrial redox imbalance. Free Radic Biol Med 38(5):644–654

Krueger KE, Srivastava S (2006) Posttranslational protein modifications: current implications for cancer detection, prevention, and therapeutics. Mol Cell Proteomics 5(10):1799–1810

Liu R, Choi J (2000) Age-associated decline in gamma-glutamylcysteine synthetase gene expression in rats. Free Radic Biol Med 28(4):566–574

Liu H, Wang H, Shenvi S, Hagen TM, Liu RM (2004) Glutathione metabolism during aging and in Alzheimer disease. Ann N Y Acad Sci 1019:346–349

Lizarbe TR, Garcia-Rama C, Tarin C, Saura M, Calvo E, Lopez JA, Lopez-Otin C, Folgueras AR, Lamas S, Zaragoza C (2008) Nitric oxide elicits functional MMP-13 protein-tyrosine nitration during wound repair. FASEB J 22(9): 3207–3215

MacMillan-Crow LA, Crow JP, Thompson JA (1998) Peroxynitrite-mediated inactivation of manganese superoxide dismutase involves nitration and oxidation of critical tyrosine residues. Biochemistry 37(6):1613–1622

Mogford JE, Sisco M, Bonomo SR, Robinson AM, Mustoe TA (2004) Impact of aging on gene expression in a rat model of ischemic cutaneous wound healing. J Surg Res 118(2):190–196

Morrison JP, Coleman MC, Aunan ES, Walsh SA, Spitz DR, Kregel KC (2005) Aging reduces responsiveness to BSO- and heat stress-induced perturbations of glutathione and antioxidant enzymes. Am J Physiol Regul Integr Comp Physiol 289(4):R1035–R1041

Mustoe TA, O'Shaughnessy K, Kloeters O (2006) Chronic wound pathogenesis and current treatment strategies: a unifying hypothesis. Plast Reconstr Surg 117(7 Suppl):35S–41S

Paglia DE, Valentine WN (1967) Studies on the quantitative and qualitative characterization of erythrocyte glutathione peroxidase. J Lab Clin Med 70(1):158–169

Radi R, Beckman JS, Bush KM, Freeman BA (1991) Peroxynitrite-induced membrane lipid peroxidation: the cytotoxic potential of superoxide and nitric oxide. Arch Biochem Biophys 288(2):481–487

Salgo MG, Bermudez E, Squadrito GL, Pryor WA (1995a) Peroxynitrite causes DNA damage and oxidation of thiols in rat thymocytes [corrected]. Arch Biochem Biophys 322(2):500–505

Salgo MG, Squadrito GL, Pryor WA (1995b) Peroxynitrite causes apoptosis in rat thymocytes. Biochem Biophys Res Commun 215(3):1111–1118

Seelig GF, Simondsen RP, Meister A (1984) Reversible dissociation of gamma-glutamylcysteine synthetase into two subunits. J Biol Chem 259(15):9345–9347

Sen CK (2003) The general case for redox control of wound repair. Wound Repair Regen 11(6):431–438

Sohal RS, Ku HH, Agarwal S, Forster MJ, Lal H (1994) Oxidative damage, mitochondrial oxidant generation and antioxidant defenses during aging and in response to food restriction in the mouse. Mech Ageing Dev 74(1–2):121–133

Soybir OC, Gurdal SO, Oran ES, Tulubas F, Yuksel M, Akyildiz AI, Bilir A, Soybir GR (2012) Delayed cutaneous wound healing in aged rats compared to younger ones. Int Wound J 9(5):478–487

Swift ME, Burns AL, Gray KL, DiPietro LA (2001) Age-related alterations in the inflammatory response to dermal injury. J Invest Dermatol 117(5):1027–1035

Szczesny B, Bhakat KK, Mitra S, Boldogh I (2004) Age-dependent modulation of DNA repair enzymes by covalent modification and subcellular distribution. Mech Ageing Dev 125(10–11):755–765

Tu Z, Anders MW (1998) Expression and characterization of human glutamate-cysteine ligase. Arch Biochem Biophys 354(2):247–254

Wu L, Brucker M, Gruskin E, Roth SI, Mustoe TA (1997) Differential effects of platelet-derived growth factor BB in accelerating wound healing in aged versus young animals: the impact of tissue hypoxia. Plast Reconstr Surg 99(3):815–822, discussion 823–814

Wu L, Xia YP, Roth SI, Gruskin E, Mustoe TA (1999) Transforming growth factor-beta1 fails to stimulate wound healing and impairs its signal transduction in an aged ischemic ulcer model: importance of oxygen and age. Am J Pathol 154(1):301–309

Zelko IN, Mariani TJ, Folz RJ (2002) Superoxide dismutase multigene family: a comparison of the CuZn-SOD (SOD1), Mn-SOD (SOD2), and EC-SOD (SOD3) gene structures, evolution, and expression. Free Radic Biol Med 33(3):337–349